

## Modal-based mixed vibration control for uncertain piezoelectric flexible structures

Yalan Xu<sup>\*1</sup>, Yu Qian<sup>1</sup>, Jianjun Chen<sup>1</sup> and Gangbing Song<sup>2</sup>

<sup>1</sup>*School of Electronic & Mechanical Engineering, Xidian University, Xi'an 710071, PR China*

<sup>2</sup>*Department of Mechanical Engineering, University of Houston, Houston, TX 77004, USA*

*(Received February 24, 2014, Revised February 20, 2015, 2015, Accepted June 20, 2015)*

**Abstract.** *H*-infinity norm relates to the maximum in the frequency response function and H-infinity control method focuses on the case that the vibration is excited at the fundamental frequency, while 2-norm relates to the output energy of systems with the input of pulses or white noises and 2-norm control method weighs the overall vibration performance of systems. The trade-off between the performance in frequency-domain and that in time-domain may be achieved by integrating two indices in the mixed vibration control method. Based on the linear fractional state space representation in the modal space for a piezoelectric flexible structure with uncertain modal parameters and un-modeled residual high-frequency modes, a mixed dynamic output feedback control design method is proposed to suppress the structural vibration. Using the linear matrix inequality (LMI) technique, the initial populations are generated by the designing of robust control laws with different *H*-infinity performance indices before the robust 2-norm performance index of the closed-loop system is included in the fitness function of optimization. A flexible beam structure with a piezoelectric sensor and a piezoelectric actuator are used as the subject for numerical studies. Compared with the velocity feedback control method, the numerical simulation results show the effectiveness of the proposed method.

**Keywords:** uncertain structures; LMI; mixed vibration control; modal space; fitness function

---

### 1. Introduction

Flexible structures have found many applications in aerospace, civil, and mechanical fields, such as large space structures, tall buildings, and flexible manipulators. The flexibility of these structures often results in structural vibration, which may last for a long time, if not suppressed in time. The light-weight flexible structures are typically characterized by poorly damped and clustered vibration modes with low resonant frequencies (Gawronski 1996). Such structures even become unstable since their open-loop poles are very close to the imaginary axis in the complex plane. Therefore, it is desirable to use active vibration control methods to attenuate the vibration of the structures to improve the structural performances. Recently, piezoelectric materials become very popular in the structural control problems due to their lightweight, large linear range and broad bandwidth. In literatures, active vibration control of structures with piezoelectric materials has been

---

\*Corresponding author, Ph.D., E-mail: [ylxu@mail.xidian.edu.cn](mailto:ylxu@mail.xidian.edu.cn)

extensively studied (Gao and Chen 2003, Song and Sethi 2006, Belouettar and Azrar 2008, Qiu and Wu 2009, Bruant and Gallimard 2010, Tavakolpour *et al.* 2010, Lin and Zhang 2012, Damanpack *et al.* 2013).

In the designing of active vibration controller, model reduction, such as balanced reduction and direct mode truncation is often required since it is difficult to implement a high-order controller for a flexible structure with a large number of vibration modes. Due to the unclear characteristics of vibration modes in the balanced-reduction model, the direct mode truncation is the common practice to obtain a relatively low-order model in the vibration control. As a result, model errors coming from the mode truncation have to be considered in order to avoid control spillover and observation spillover. The interaction of two spillovers may lead to system instability, especially in the non-collocated control. To deal with the problem, a variety of control design frameworks have been explored (Balas 1978, Meirovitch and Baruh 1983, Vasques and Rodrigues 2006, Morales *et al.* 2012). In addition, the variation in modal parameters (resonant frequencies and damping ratio) may degrade the performance of the controller (Bala 1995, Zhang and Shao 2001, Samuel and Vicente 2006, Chen *et al.* 2007, Gasbarri *et al.* 2014).

It is well known that each robust control method is mainly useful for capturing a set of design specifications. Robust  $H_\infty$  control method focuses on the case that the vibration is excited at the fundamental frequency and tends to be conservative and cost-wasting since the  $H_\infty$  norm relates to the maximum in the frequency response function. The  $H_2$  norm relates to the output energy of a system with the input of pulses or white noises, and, as a result, the robust  $H_2$  control method takes the overall performance of a system into account without considering the fundamental resonance excited by the external disturbance. Two norm indices should be integrated to achieve the trade-off between the robust performance and time domain performance in the structural vibration control. Most of the studies available focus on the state feedback controller or observer-based feedback controllers of structural systems (Yang and Sun 2002, Caracciolo *et al.* 2005, Karimi *et al.* 2008, Rittenschober and Schlacher 2012, Schulz *et al.* 2013). In practice, the measurement of the modal displacement and velocity is not practical for vibration control of engineering structure and an observer-based controller may require a large number of computation.

In this paper, a mixed dynamical output feedback control law is designed by not only minimizing the  $H_2$  norm but also setting an upper bound on  $H_\infty$  norm to suppress the vibration of uncertain piezoelectric flexible structures due to external disturbances. The contribution of this paper is to provide a design method for the mixed dynamic output feedback controller using linear matrix inequality (LMI) and genetic algorithm, in which the robust  $H_2$  performance index of the closed-loop system with norm-bound uncertainty is chosen in the fitness function, which has not dealt with by the researchers to the best of authors' knowledge. The remainder of this paper is organized as follows. First, the linear fractional representation (LFR) and its state space representation in the modal space for uncertain piezoelectric flexible structures are given, taking into account uncertain modal parameters and un-modeled residual high-frequency modes. Then, the procedures of the mixed dynamic output feedback control design are given. In the optimization processing of genetic algorithm, the initial populations are generated by the designing of  $H_\infty$  suboptimal controllers with different  $H_\infty$  performance indices and the robust  $H_2$  performance of system is chosen in the fitness function. Finally, compared to the velocity feedback control method, numerical simulation results are given to demonstrate the effectiveness of the proposed method.

## 2. Modal state space representation

### 2.1 Deterministic modal state space modeling

Considering a flexible structure with  $K$  piezoelectric actuator patches and  $L$  piezoelectric sensor patches in the modal space and including  $m$  modes in the model, we have (Xu and Chen 2008)

$$\ddot{q}_i(t) + 2\xi_i\omega_i\dot{q}_i(t) + \omega_i^2q_i(t) = \sum_{j=1}^K b_{ij}V_{aj}(t) + \sum_{j=1}^L \tilde{b}_{ij}w_j(t), \quad i = 1, 2, \dots, m \quad (1)$$

where  $q_i(t)$  is the  $i$ th modal coordinate.  $\xi_i$ ,  $\omega_i$  are the frequency and damping ratio of the  $i$ th mode respectively.  $V_{aj}(t)$  is the voltage applied to the  $j$ th actuator;  $b_{ij}$  is the influence coefficient of  $V_{aj}(t)$  on the  $i$ th mode.  $w_j(t)$  is the  $j$ th external disturbance.  $\tilde{b}_{ij}$  is the influence coefficient of  $w_j(t)$  on the  $i$ th mode.

The performance and measured outputs  $y_p(t)$ ,  $z_l(t)$  ( $p=1, 2, \dots, P$ ;  $l=1, 2, \dots, L$ ) can be respectively defined by the modal displacement as follows

$$y_p(t) = \sum_{j=1}^m c_{pj}q_j(t), \quad z_l(t) = \sum_{j=1}^m \tilde{c}_{lj}q_j(t) \quad (2)$$

where  $c_{pj}$  is the influence coefficient of the  $j$ th mode on  $y_p(t)$ , and  $\tilde{c}_{lj}$  is the influence coefficient of the  $j$ th mode on  $z_l(t)$ .

Defining the state vector  $\mathbf{x}(t)=[q_1(t), \dot{q}_1(t), q_2(t), \dot{q}_2(t), \dots, q_m(t), \dot{q}_m(t)]^T$ , the state space model of the structure can be written as

$$\begin{aligned} \dot{\mathbf{x}}(t) &= \mathbf{A}\mathbf{x}(t) + \mathbf{B}\mathbf{V}_a(t) + \tilde{\mathbf{B}}\mathbf{w}(t) \\ \mathbf{y}(t) &= \mathbf{C}\mathbf{x}(t), \quad \mathbf{z}(t) = \tilde{\mathbf{C}}\mathbf{x}(t) \end{aligned} \quad (3)$$

where,  $\mathbf{y}(t)$  is the performance output vector.  $\mathbf{z}(t)$  is the measured output vector.  $\mathbf{V}_a(t)=[V_{a1}(t), V_{a2}(t), \dots, V_{aK}(t)]^T$  is the control input vector.  $\mathbf{w}(t)=[w_1(t), w_2(t), \dots, w_L(t)]^T$  is the external disturbance vector.  $\mathbf{A} = \text{diag}\{\mathbf{A}_1 \quad \dots \quad \mathbf{A}_i \quad \dots \quad \mathbf{A}_m\}$ ,  $\mathbf{A}_i = \begin{bmatrix} 0 & 1 \\ -\omega_i^2 & -2\xi_i\omega_i \end{bmatrix}$ .

### 2.2 Uncertain modal state space modeling

In the uncertain model, the variation of modal parameters and residual modes should be included. The variations  $\Delta\omega_i$ ,  $\Delta\xi_i$  of the  $i$ th modal frequency and damping ratio can be expressed as

$$\Delta\omega_i = \omega_{\Delta i}\delta_{1i}, \quad \Delta\xi_i = \xi_{\Delta i}\delta_{2i} \quad (4)$$

where  $\|\delta_{1i}\| \leq 1$ ,  $\|\delta_{2i}\| \leq 1$ . As a result, we have

$$\hat{\mathbf{A}}_i = \begin{bmatrix} 0 & 1 \\ -\hat{\omega}_i^2 & -2\hat{\xi}_i\hat{\omega}_i \end{bmatrix} \quad (5)$$

where  $\hat{\omega}_i = \omega_i + \Delta\omega_i$ ,  $\hat{\xi}_i = \xi_i + \Delta\xi_i$ . Substituting Eq. (4) into Eq. (5) and neglecting the high-order small terms, we have

$$\begin{aligned} \hat{\mathbf{A}}_i &= \mathbf{A}_i + \mathbf{E}_i \boldsymbol{\delta}_i \mathbf{F}_i, \quad \boldsymbol{\delta}_i = \text{diag} \{ \delta_{1i}, \delta_{2i} \} \\ \mathbf{E}_i &= \begin{bmatrix} 0 & 0 \\ -\omega_{\Delta i} & -\xi_{\Delta i} \end{bmatrix}, \quad \mathbf{F}_i = \begin{bmatrix} 2\omega_i & 2\xi_i \\ 0 & 2\omega_i \end{bmatrix} \end{aligned} \quad (6)$$

As a result, the uncertain system matrix  $\hat{\mathbf{A}}$  can be obtained by

$$\begin{aligned} \hat{\mathbf{A}} &= \text{diag} \{ \hat{\mathbf{A}}_1, \dots, \hat{\mathbf{A}}_i, \dots, \hat{\mathbf{A}}_m \} = \mathbf{A} + \mathbf{E} \boldsymbol{\Delta}_1 \mathbf{F}, \quad \|\boldsymbol{\Delta}_1\|_1 \leq 1 \\ \mathbf{A} &= \text{diag} \{ \mathbf{A}_1, \dots, \mathbf{A}_i, \dots, \mathbf{A}_m \}, \quad \boldsymbol{\Delta}_1 = \text{diag} \{ \boldsymbol{\delta}_1, \dots, \boldsymbol{\delta}_i, \dots, \boldsymbol{\delta}_m \} \\ \mathbf{E} &= \text{diag} \{ \mathbf{E}_1, \dots, \mathbf{E}_i, \dots, \mathbf{E}_m \}, \quad \mathbf{F} = \text{diag} \{ \mathbf{F}_1, \dots, \mathbf{F}_i, \dots, \mathbf{F}_m \} \end{aligned} \quad (7)$$

The model error due to residual high-frequency modes is represented by norm-bound addition uncertainty  $\Delta G(s)$  and we have

$$\begin{aligned} \hat{G}(s) &= G(s) + \Delta G(s) \\ \Delta G(s) &= W(s) \cdot \Delta_2, \quad \|\Delta_2\|_\infty \leq 1 \end{aligned} \quad (8)$$

where,  $\Delta_2$  is the unknown uncertainty.  $W(s)$  is determined by the upper bound of residual high-frequency modes.

The state-space representation for  $W(s)$  can be written as

$$\begin{aligned} \dot{\mathbf{x}}_r(t) &= \mathbf{A}_r \mathbf{x}_r(t) + \mathbf{B}_r \mathbf{V}_a(t) \\ \mathbf{h}_2(t) &= \mathbf{C}_r \mathbf{x}_r(t) + \mathbf{D}_r \mathbf{V}_a(t) \end{aligned} \quad (9)$$

where,  $\mathbf{x}_r(t)$  is the state vector;  $\mathbf{V}_a(t)$  is the control input vector;  $\mathbf{h}_2(t)$  is the output vector;  $\mathbf{A}_r$ ,  $\mathbf{B}_r$ ,  $\mathbf{C}_r$ ,  $\mathbf{D}_r$  are the matrices corresponding to the chosen transfer function  $\mathbf{w}(s)$  for the normalization of the uncertainty, which forms the upper bound in the un-modeled high-frequency region (Sana and Rao 2000).

With Eq. (3), Eq. (7) and Eq. (9), the linear fractional representation (LFR) for the uncertain piezoelectric flexible structure is shown in Fig. 1. The corresponding state-space representation for  $\hat{G}(s)$  can be written as

$$\begin{aligned} \dot{\mathbf{x}}_o(t) &= \mathbf{A}_o \mathbf{x}_o(t) + \mathbf{B}_o \mathbf{V}_a(t) + \tilde{\mathbf{B}}_o \mathbf{w}(t) + \mathbf{E}_1 \mathbf{g}(t) \\ \mathbf{y}(t) &= \mathbf{C}_o \mathbf{x}_o(t) + \mathbf{E}_2 \mathbf{g}(t) \\ \mathbf{z}(t) &= \tilde{\mathbf{C}}_o \mathbf{x}_o(t) + \mathbf{E}_3 \mathbf{g}(t) \\ \mathbf{h}(t) &= \mathbf{F}_1 \mathbf{x}_o(t) + \mathbf{F}_2 \mathbf{V}_a(t) \\ \mathbf{g}(t) &= \boldsymbol{\Delta} \mathbf{h}(t) \\ \|\boldsymbol{\Delta}\|_\infty &\leq 1 \end{aligned} \quad (10)$$

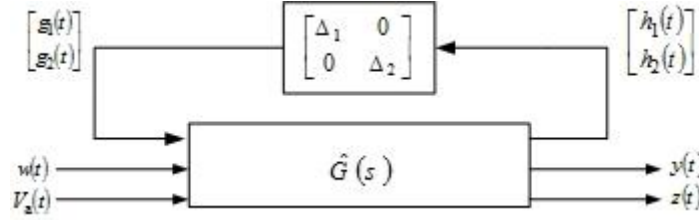


Fig. 1 LFR for uncertain flexible structures

where,  $\mathbf{x}_o(t) = \begin{Bmatrix} \dot{\mathbf{x}}(t) \\ \mathbf{x}_r(t) \end{Bmatrix}$ ,  $\mathbf{A}_o = \begin{bmatrix} \mathbf{A} & \mathbf{0} \\ \mathbf{0} & \mathbf{A}_r \end{bmatrix}$ ,  $\mathbf{B}_o = \begin{bmatrix} \mathbf{B} \\ \mathbf{B}_r \end{bmatrix}$ ,  $\mathbf{C}_o = \begin{bmatrix} \mathbf{C}^T \\ \mathbf{0} \end{bmatrix}$ ,  $\tilde{\mathbf{B}}_o = \begin{bmatrix} \tilde{\mathbf{B}} \\ \mathbf{0} \end{bmatrix}$ ,  $\tilde{\mathbf{C}}_o = \begin{bmatrix} \tilde{\mathbf{C}} \\ \mathbf{0} \end{bmatrix}$ ,  $\mathbf{E}_1 = \begin{bmatrix} \mathbf{E}^T \\ \mathbf{0} \end{bmatrix}$ ,  $\mathbf{E}_2 = \begin{bmatrix} \mathbf{0} \\ \mathbf{E}_y \end{bmatrix}$ ,  $\mathbf{E}_3 = \begin{bmatrix} \mathbf{0} \\ \mathbf{E}_z \end{bmatrix}$ ,  $\mathbf{F}_1 = \begin{bmatrix} \mathbf{F} & \mathbf{0} \\ \mathbf{0} & \mathbf{C}_r \end{bmatrix}$ ,  $\mathbf{F}_2 = \begin{bmatrix} \mathbf{0} \\ \mathbf{D}_r \end{bmatrix}$ ,  $\mathbf{g}(t) = \begin{Bmatrix} \mathbf{g}_1(t) \\ \mathbf{g}_2(t) \end{Bmatrix}$ ,  $\mathbf{h}(t) = \begin{Bmatrix} \mathbf{h}_1(t) \\ \mathbf{h}_2(t) \end{Bmatrix}$ ,  $\Delta = \begin{bmatrix} \Delta_1 & \mathbf{0} \\ \mathbf{0} & \Delta_2 \end{bmatrix}$ .

### 3. Dynamic output feedback law

The following dynamic output feedback control law is applied to the open-loop structure Eq. (10)

$$\dot{\boldsymbol{\zeta}}(t) = \mathbf{A}_k \boldsymbol{\zeta}(t) + \mathbf{B}_k \mathbf{z}(t), \quad \mathbf{V}_a(t) = \mathbf{C}_k \boldsymbol{\zeta}(t) \quad (11)$$

where,  $\boldsymbol{\zeta}(t)$  is the state vector of the controller.  $\mathbf{A}_k$ ,  $\mathbf{B}_k$ ,  $\mathbf{C}_k$  are unknown parameters of the controller. As a result, the state space realization of the closed-loop system is written as

$$\begin{aligned} \dot{\hat{\mathbf{x}}}(t) &= \mathbf{A}_c \hat{\mathbf{x}}(t) + \mathbf{B}_{cw} \mathbf{w}(t) + \mathbf{E}_{cx} \mathbf{g}(t) \\ \mathbf{y}(t) &= \mathbf{C}_c \hat{\mathbf{x}}(t) + \mathbf{E}_{cy} \mathbf{g}(t) \\ \mathbf{h}(t) &= \mathbf{F}_{cx} \hat{\mathbf{x}}(t) + \mathbf{F}_{cg} \mathbf{g}(t) \\ \mathbf{g}(t) &= \Delta \mathbf{h}(t) \\ \|\Delta\|_\infty &\leq 1 \end{aligned} \quad (12)$$

where,  $\hat{\mathbf{x}}(t) = \begin{Bmatrix} \mathbf{x}_o(t) \\ \boldsymbol{\zeta}(t) \end{Bmatrix}$ ,  $\mathbf{A}_c = \begin{bmatrix} \mathbf{A}_o + \mathbf{B}_o \mathbf{D}_k \tilde{\mathbf{C}}_o & \mathbf{B}_o \mathbf{C}_k \\ \mathbf{B}_k \tilde{\mathbf{C}}_o & \mathbf{A}_k \end{bmatrix}$ ,  $\mathbf{B}_{cw} = \begin{bmatrix} \tilde{\mathbf{B}}_o \\ \mathbf{0} \end{bmatrix}$ ,  $\mathbf{C}_c = \begin{bmatrix} \mathbf{C}_o^T \\ \mathbf{0} \end{bmatrix}$ ,  $\mathbf{E}_{cx} = \begin{bmatrix} \mathbf{E}_1 + \mathbf{B}_o \mathbf{D}_k \mathbf{E}_3 \\ \mathbf{B}_k \mathbf{E}_3 \end{bmatrix}$ ,  $\mathbf{E}_{cy} = \mathbf{E}_2$ ,  $\mathbf{F}_{cx} = \begin{bmatrix} \mathbf{F}_1 + \mathbf{F}_2 \mathbf{D}_k \tilde{\mathbf{C}}_o & \mathbf{F}_2 \mathbf{C}_k \end{bmatrix}$ ,  $\mathbf{F}_{cg} = \mathbf{F}_2 \mathbf{D}_k \mathbf{E}_3$ .

### 4. Mixed vibration control of uncertain structure

Genetic algorithm is an optimization and search technique based on the principles of genetic and natural selection, which is an adaptive method used to solve search and optimization problems (Fogel 1994, Tavakolpour *et al.* 2010, Xu and Ou 2013). Our aim is to use the linear matrix

inequality and genetic algorithm approach for seeking the best controller parameters in mixed  $H_2/H_\infty$  control design. The steps of genetic algorithm based dynamic output feedback control by using LMI are provided in this section.

#### 4.1 Encoding

When genetic algorithm is applied to solve a practical problem, the parameter set of the problem first needs to be coded as a finite-length string. In the present study, we use a real-coded genetic algorithm. Thus, every chromosome is a string of real values. Here, the real coding is used to represent the solution  $[\mathbf{P}_k, \mathbf{A}_k, \mathbf{B}_k, \mathbf{C}_k]$  to the dynamic output feedback controller Eq. (11).

#### 4.2 Initial population

The initial populations  $P_j = \{\mathbf{A}_k, \mathbf{B}_k, \mathbf{C}_k\}$ ,  $j=1,2,\dots, N$  ( $N$  is the size of populations) are generated by the designing of  $H_\infty$  suboptimal controllers with different  $H_\infty$  performance indices (Xu and Chen 2008). For the uncertain closed system Eq. (12) with the norm-bound uncertainties  $\mathbf{g}^T(t)\mathbf{g}(t) \leq \mathbf{h}^T(t)\mathbf{h}(t)$ , its robust stability and disturbance rejection can be guaranteed if the following condition can be satisfied

$$\begin{aligned} dV(\hat{\mathbf{x}}(t))/dt + \mathbf{y}^T(t)\mathbf{y}(t) - \gamma^2 \mathbf{w}^T(t)\mathbf{w}(t) &< 0 \\ V(\hat{\mathbf{x}}(t)) = \hat{\mathbf{x}}^T(t)\mathbf{P}\hat{\mathbf{x}}(t) &> 0, \mathbf{P}^T = \mathbf{P} > 0 \end{aligned} \quad (13)$$

where  $\gamma$  is the upper bound on the  $H_\infty$  norm from  $w(t)$  to  $y(t)$  of the system. As a result, the norm-bound uncertainties and the condition for the disturbance rejection with robust stability can be respectively expressed as

$$\begin{bmatrix} \hat{\mathbf{x}}(t) \\ \mathbf{g}(t) \\ \mathbf{w}(t) \end{bmatrix}^T \begin{bmatrix} -\mathbf{F}_{cx}^T \mathbf{F}_{cx} & -\mathbf{F}_{cx}^T \mathbf{F}_{cg} & \mathbf{0} \\ -\mathbf{F}_{cg}^T \mathbf{F}_{cx} & \mathbf{I} - \mathbf{F}_{cg}^T \mathbf{F}_{cg} & \mathbf{0} \\ \mathbf{0} & \mathbf{0} & \mathbf{0} \end{bmatrix} \begin{bmatrix} \hat{\mathbf{x}}(t) \\ \mathbf{g}(t) \\ \mathbf{w}(t) \end{bmatrix} \leq 0 \quad (14)$$

$$\begin{bmatrix} \hat{\mathbf{x}}(t) \\ \mathbf{g}(t) \\ \mathbf{w}(t) \end{bmatrix}^T \begin{bmatrix} \mathbf{A}_c^T \mathbf{P} + \mathbf{P} \mathbf{A}_c + \mathbf{C}_c^T \mathbf{C}_c & \mathbf{P} \mathbf{E}_{cx} + \mathbf{C}_c^T \mathbf{E}_{cy} & \mathbf{P} \mathbf{B}_{cw} \\ \mathbf{E}_{cx}^T \mathbf{P} + \mathbf{E}_{cy}^T \mathbf{C}_c & \mathbf{E}_{cy}^T \mathbf{E}_{cy} & \mathbf{0} \\ \mathbf{B}_{cw}^T \mathbf{P} & \mathbf{0} & -\gamma^2 \mathbf{I} \end{bmatrix} \begin{bmatrix} \hat{\mathbf{x}}(t) \\ \mathbf{g}(t) \\ \mathbf{w}(t) \end{bmatrix} < 0 \quad (15)$$

Using  $S$ -procedure, the robust stability and disturbance rejection can be guaranteed for the system with norm-bound uncertainties if the following condition can be satisfied

$$\begin{bmatrix} \mathbf{A}_c^T \mathbf{P} + \mathbf{P} \mathbf{A}_c + \mathbf{C}_c^T \mathbf{C}_c + \beta \mathbf{F}_{cx}^T \mathbf{F}_{cx} & \mathbf{P} \mathbf{E}_{cx} + \mathbf{C}_c^T \mathbf{E}_{cy} + \beta \mathbf{F}_{cx}^T \mathbf{F}_{cg} & \mathbf{P} \mathbf{B}_{cw} \\ \mathbf{E}_{cx}^T \mathbf{P} + \mathbf{E}_{cy}^T \mathbf{C}_c + \beta \mathbf{F}_{cg}^T \mathbf{F}_{cx} & \mathbf{E}_{cy}^T \mathbf{E}_{cy} + \beta \mathbf{F}_{cg}^T \mathbf{F}_{cg} - \beta \mathbf{I} & \mathbf{0} \\ \mathbf{B}_{cw}^T \mathbf{P} & \mathbf{0} & -\gamma^2 \mathbf{I} \end{bmatrix} < 0, \beta \geq 0 \quad (16)$$

Defining a matrix set  $\tilde{S} = \{\text{diag}\{\tilde{\mathbf{S}}_1, \dots, \tilde{\mathbf{S}}_m, \tilde{s}\}; \tilde{\mathbf{S}}_i = R^{2 \times 2}, \tilde{s} = R, \tilde{\mathbf{S}}_i > 0, \tilde{s} > 0\}$  and reducing the conservative of design, the disturbance of the uncertain system can be rejected with robust stability

if the following condition is satisfied

$$\begin{bmatrix} \mathbf{A}_c^T \mathbf{P} + \mathbf{P} \mathbf{A}_c + \mathbf{C}_c^T \mathbf{C}_c + \mathbf{F}_{cx}^T \mathbf{S} \mathbf{F}_{cx} & \mathbf{P} \mathbf{E}_{cx} + \mathbf{C}_c^T \mathbf{E}_{cy} + \mathbf{F}_{cx}^T \mathbf{S} \mathbf{F}_{cg} & \mathbf{P} \mathbf{B}_{cw} \\ \mathbf{E}_{cx}^T \mathbf{P} + \mathbf{E}_{cy}^T \mathbf{C}_c + \mathbf{F}_{cg}^T \mathbf{S} \mathbf{F}_{cx} & \mathbf{E}_{cy}^T \mathbf{E}_{cy} + \mathbf{F}_{cg}^T \mathbf{S} \mathbf{F}_{cg} - \mathbf{S} & \mathbf{0} \\ \mathbf{B}_{cw}^T \mathbf{P} & \mathbf{0} & -\gamma^2 \mathbf{I} \end{bmatrix} < 0 \quad (17)$$

Using Schur complement, Eq. (17) can be rewritten as

$$\begin{bmatrix} \mathbf{P} \mathbf{A}_c + \mathbf{A}_c^T \mathbf{P} & \mathbf{P} \mathbf{E}_{cx} & \mathbf{P} \mathbf{B}_{cw} & \mathbf{F}_{cx}^T & \mathbf{C}_c^T \\ & -\mathbf{S} & \mathbf{0} & \mathbf{F}_{cg}^T & \mathbf{E}_{cy}^T \\ & & -\gamma^2 \mathbf{I} & \mathbf{0} & \mathbf{0} \\ \text{sym} & & & -\mathbf{S}^{-1} & \mathbf{0} \\ & & & & -\mathbf{I} \end{bmatrix} < 0 \quad (18)$$

Conducting the Partitioning  $\mathbf{P} = \begin{bmatrix} \mathbf{p}_1 & \mathbf{p}_2 \\ \mathbf{p}_2^T & \mathbf{p}_3 \end{bmatrix}$  and  $\mathbf{P}^{-1} = \begin{bmatrix} \hat{\mathbf{p}}_1 & \hat{\mathbf{p}}_2 \\ \hat{\mathbf{p}}_2^T & \hat{\mathbf{p}}_3 \end{bmatrix}$ , and performing a congruence

transformation with  $\text{diag}\{\hat{\mathbf{F}}_1, \mathbf{I}, \mathbf{I}, \mathbf{I}, \mathbf{I}\}$  ( $\hat{\mathbf{F}}_1 = \begin{bmatrix} \hat{\mathbf{p}}_1 & \mathbf{I} \\ \hat{\mathbf{p}}_2^T & \mathbf{0} \end{bmatrix}$ ) on Eq. (18), the nonlinear matrix inequality Eq. (18) can be converted into the following linear matrix inequality

$$\begin{bmatrix} \mathbf{A}_o \hat{\mathbf{p}}_1 + \hat{\mathbf{p}}_1 \mathbf{A}_o^T + \mathbf{B}_o \mathbf{C}_M + \mathbf{C}_M^T \mathbf{B}_o^T & \mathbf{A}_o + \mathbf{B}_o \mathbf{D}_k \tilde{\mathbf{C}}_o + \mathbf{A}_M^T & \mathbf{E}_1 + \mathbf{B}_o \mathbf{D}_k \mathbf{E}_3 & \tilde{\mathbf{B}}_o & \hat{\mathbf{p}}_1 \mathbf{F}_1^T + \mathbf{C}_M^T \mathbf{F}_2^T & \hat{\mathbf{p}}_1 \mathbf{C}_o^T \\ & \mathbf{A}_o^T \hat{\mathbf{p}}_1 + \hat{\mathbf{p}}_1 \mathbf{A}_o + \tilde{\mathbf{C}}_o^T \mathbf{B}_M^T + \mathbf{B}_M \tilde{\mathbf{C}}_o & \mathbf{p}_1 \mathbf{E}_1 + \mathbf{B}_M \mathbf{E}_3 & \mathbf{p}_1 \tilde{\mathbf{B}}_o & \mathbf{F}_1^T + \tilde{\mathbf{C}}_o \mathbf{D}_k^T \mathbf{F}_2^T & \mathbf{C}_o^T \\ & & -\mathbf{S} & \mathbf{0} & \mathbf{E}_3^T \mathbf{D}_k^T \mathbf{F}_2^T & \mathbf{E}_2^T \\ \text{sym} & & & -\gamma^2 \mathbf{I} & \mathbf{0} & \mathbf{0} \\ & & & & -\mathbf{S}^{-1} & \mathbf{0} \\ & & & & & -\mathbf{I} \end{bmatrix} < 0 \quad (19)$$

where,  $\mathbf{A}_M = \mathbf{p}_1 (\mathbf{A}_o + \mathbf{B}_o \mathbf{D}_k \tilde{\mathbf{C}}_o) \hat{\mathbf{p}}_1 + \mathbf{p}_2 \mathbf{B}_k \tilde{\mathbf{C}}_o \hat{\mathbf{p}}_1 + \mathbf{p}_1 \mathbf{B}_o \mathbf{C}_k \hat{\mathbf{p}}_2^T + \mathbf{p}_2 \mathbf{A}_k \hat{\mathbf{p}}_2^T$ ,  $\mathbf{B}_M = \mathbf{p}_1 \mathbf{B}_o \mathbf{D}_k + \mathbf{p}_2 \mathbf{B}_k$ ,  $\mathbf{C}_M = \mathbf{D}_k \tilde{\mathbf{C}}_o \hat{\mathbf{p}}_1 + \mathbf{C}_k \hat{\mathbf{p}}_2^T$ ,  $\mathbf{p}_2 \hat{\mathbf{p}}_2 = \mathbf{I} - \mathbf{p}_1 \hat{\mathbf{p}}_1$ .

#### 4.3 Fitness function

Fitness function in genetic algorithm is used to evaluate the goodness of a solution. The better solution has a higher fitness value. The fitness function is calculated using the following equation (Tavakolpour *et al* 2010)

$$f(j) = M - J_i \quad (20)$$

where,  $M$  is be assigned a large positive value, and it is chosen to guarantee that the value of the fitness function is always positive,  $J_i$  is the introduced performance index of the  $j$ th individual. The

objective of the control system in this work is to minimize  $H_2$  norm accompanied by setting an upper bound on  $H_\infty$  norm to avoid the worst vibration situation. So, the robust  $H_2$  performance index of the closed-loop system with norm-bound uncertainty will be chosen in the fitness function.

$H_2$  norm relates to the output energy of system with pulses or white noises as the input, in which the external disturbance is taken as the impulse excitation and Gauss white noises random process. As a result, for zero initial conditions and given disturbance  $w(t)=w_0\delta(t)$ , the energy of system can be defined as

$$\hat{J}_2 = \int_0^\infty \mathbf{y}^T(t)\mathbf{y}(t)dt \quad (21)$$

Hence, the robust  $H_2$  performance index with norm-bound uncertainty can be defined as

$$J_2 = \sup_{w_0, \Delta} \left\{ \int_0^\infty \mathbf{y}^T(t)\mathbf{y}(t)dt : \|w_0\| \leq 1, \|\Delta\|_\infty \leq 1 \right\} \quad (22)$$

Since  $\hat{\mathbf{x}}(0)=0, w(t)=w_0\delta(t)$  is equivalent to  $\hat{\mathbf{x}}(0)=\mathbf{B}_{cw}w_0, \mathbf{w}(t)=\mathbf{0}$ , Eq. (12) can be written as

$$\begin{aligned} \dot{\hat{\mathbf{x}}}(t) &= \mathbf{A}_c \hat{\mathbf{x}}(t) + \mathbf{E}_{cx} \mathbf{g}(t) \\ \mathbf{y}(t) &= \mathbf{C}_c \hat{\mathbf{x}}(t) + \mathbf{E}_{cy} \mathbf{g}(t) \\ \mathbf{h}(t) &= \mathbf{F}_{cx} \hat{\mathbf{x}}(t) + \mathbf{F}_{cg} \mathbf{g}(t) \\ \mathbf{g}(t) &= \Delta \mathbf{h}(t), \|\Delta\|_\infty \leq 1 \end{aligned} \quad (23)$$

Therefore, the norm-bound uncertainty and robust stability condition can be respectively expressed as

$$\begin{aligned} \mathbf{g}^T(t)\mathbf{g}(t) - \mathbf{h}^T(t)\mathbf{h}(t) &= \mathbf{g}^T(t)\mathbf{g}(t) - (\mathbf{F}_{cx} \hat{\mathbf{x}}(t) + \mathbf{F}_{cg} \mathbf{g}(t))^T (\mathbf{F}_{cx} \hat{\mathbf{x}}(t) + \mathbf{F}_{cg} \mathbf{g}(t)) \\ &= \begin{bmatrix} \hat{\mathbf{x}}(t) \\ \mathbf{g}(t) \end{bmatrix}^T \begin{bmatrix} -\mathbf{F}_{cx}^T \mathbf{F}_{cx} & -\mathbf{F}_{cx}^T \mathbf{F}_{cg} \\ -\mathbf{F}_{cg}^T \mathbf{F}_{cx} & \mathbf{I} - \mathbf{F}_{cg}^T \mathbf{F}_{cg} \end{bmatrix} \begin{bmatrix} \hat{\mathbf{x}}(t) \\ \mathbf{g}(t) \end{bmatrix} \leq 0 \end{aligned} \quad (24)$$

$$\begin{aligned} \mathbf{d}V(\hat{\mathbf{x}}(t))/\mathbf{d}t &= \dot{\hat{\mathbf{x}}}^T(t)\mathbf{P}\hat{\mathbf{x}}(t) + \hat{\mathbf{x}}^T(t)\mathbf{P}\dot{\hat{\mathbf{x}}}(t) \\ &= (\mathbf{A}_c \hat{\mathbf{x}}(t) + \mathbf{E}_{cx} \mathbf{g}(t))^T \mathbf{P}\hat{\mathbf{x}}(t) + \hat{\mathbf{x}}^T(t)\mathbf{P}(\mathbf{A}_c \hat{\mathbf{x}}(t) + \mathbf{E}_{cx} \mathbf{g}(t)) \\ &= \begin{bmatrix} \hat{\mathbf{x}}(t) \\ \mathbf{g}(t) \end{bmatrix}^T \begin{bmatrix} \mathbf{A}_c^T \mathbf{P} + \mathbf{P}\mathbf{A}_c & \mathbf{P}\mathbf{E}_{cx} \\ \mathbf{E}_{cx}^T \mathbf{P} & \mathbf{0} \end{bmatrix} \begin{bmatrix} \hat{\mathbf{x}}(t) \\ \mathbf{g}(t) \end{bmatrix} < 0 \end{aligned} \quad (25)$$

Using  $S$ -procedure, the robust stability condition can be expressed as

$$\begin{bmatrix} \mathbf{A}_c^T \mathbf{P} + \mathbf{P}\mathbf{A}_c + \beta \mathbf{F}_{cx}^T \mathbf{F}_{cx} & \mathbf{P}\mathbf{E}_{cx} + \beta \mathbf{F}_{cx}^T \mathbf{F}_{cg} \\ \mathbf{E}_{cx}^T \mathbf{P} + \beta \mathbf{F}_{cg}^T \mathbf{F}_{cx} & \beta \mathbf{F}_{cg}^T \mathbf{F}_{cg} - \beta \mathbf{I} \end{bmatrix} < 0, \beta \geq 0 \quad (26)$$

Further reducing the conservative of design, Eq. (26) can be written as

$$\begin{bmatrix} \mathbf{A}_c^T \mathbf{P} + \mathbf{P} \mathbf{A}_c + \mathbf{F}_{cx}^T \mathbf{S} \mathbf{F}_{cx} & \mathbf{P} \mathbf{E}_{cx} + \mathbf{F}_{cx}^T \mathbf{S} \mathbf{F}_{cg} \\ \mathbf{E}_{cx}^T \mathbf{P} + \mathbf{F}_{cg}^T \mathbf{S} \mathbf{F}_{cx} & \mathbf{F}_{cg}^T \mathbf{S} \mathbf{F}_{cg} - \mathbf{S} \end{bmatrix} < 0 \quad (27)$$

Eq. (27) can be written as

$$\begin{bmatrix} \mathbf{A}_c^T \mathbf{P} + \mathbf{P} \mathbf{A}_c & \mathbf{P} \mathbf{E}_{cx} \\ \mathbf{E}_{cx}^T \mathbf{P} & -\mathbf{S} \end{bmatrix} + \begin{bmatrix} \mathbf{F}_{cx}^T \\ \mathbf{F}_{cg}^T \end{bmatrix} [\mathbf{S}] \begin{bmatrix} \mathbf{F}_{cx} & \mathbf{F}_{cg} \end{bmatrix} < 0 \quad (28)$$

With arbitrary small  $\varepsilon > 0$ , we have

$$\begin{bmatrix} \mathbf{A}_c^T \mathbf{P} + \mathbf{P} \mathbf{A}_c & \mathbf{P} \mathbf{E}_{cx} \\ \mathbf{E}_{cx}^T \mathbf{P} & -\mathbf{S} \end{bmatrix} + \begin{bmatrix} \mathbf{F}_{cx}^T \\ \mathbf{F}_{cg}^T \end{bmatrix} [\mathbf{S}] \begin{bmatrix} \mathbf{F}_{cx} & \mathbf{F}_{cg} \end{bmatrix} + \varepsilon \begin{bmatrix} \mathbf{C}_c^T \\ \mathbf{E}_{cy}^T \end{bmatrix} \begin{bmatrix} \mathbf{C}_c & \mathbf{E}_{cy} \end{bmatrix} < 0 \quad (29)$$

With  $\hat{\mathbf{P}} = \varepsilon^{-1} \mathbf{P}$  and  $\hat{\mathbf{S}} = \varepsilon^{-1} \mathbf{S} \in \tilde{\mathcal{S}}$ , we have

$$\begin{bmatrix} \mathbf{A}_c^T \hat{\mathbf{P}} + \hat{\mathbf{P}} \mathbf{A}_c & \hat{\mathbf{P}} \mathbf{E}_{cx} \\ \mathbf{E}_{cx}^T \hat{\mathbf{P}} & -\hat{\mathbf{S}} \end{bmatrix} + \begin{bmatrix} \mathbf{F}_{cx}^T \\ \mathbf{F}_{cg}^T \end{bmatrix} [\hat{\mathbf{S}}] \begin{bmatrix} \mathbf{F}_{cx} & \mathbf{F}_{cg} \end{bmatrix} + \begin{bmatrix} \mathbf{C}_c^T \\ \mathbf{E}_{cy}^T \end{bmatrix} \begin{bmatrix} \mathbf{C}_c & \mathbf{E}_{cy} \end{bmatrix} < 0 \quad (30)$$

Using Eq. (23), Eq. (24), Eq. (25) and Eq. (30), we have

$$\begin{aligned} & \begin{bmatrix} \hat{\mathbf{x}}(t) \\ \mathbf{g}(t) \end{bmatrix}^T \left\{ \begin{bmatrix} \mathbf{A}_c^T \hat{\mathbf{P}} + \hat{\mathbf{P}} \mathbf{A}_c & \hat{\mathbf{P}} \mathbf{E}_{cx} \\ \mathbf{E}_{cx}^T \hat{\mathbf{P}} & -\hat{\mathbf{S}} \end{bmatrix} + \begin{bmatrix} \mathbf{F}_{cx}^T \\ \mathbf{F}_{cg}^T \end{bmatrix} [\hat{\mathbf{S}}] \begin{bmatrix} \mathbf{F}_{cx} & \mathbf{F}_{cg} \end{bmatrix} + \begin{bmatrix} \mathbf{C}_c^T \\ \mathbf{E}_{cy}^T \end{bmatrix} \begin{bmatrix} \mathbf{C}_c & \mathbf{E}_{cy} \end{bmatrix} \right\} \begin{bmatrix} \hat{\mathbf{x}}(t) \\ \mathbf{g}(t) \end{bmatrix} \\ & = \dot{V}(\hat{\mathbf{x}}(t)) - \mathbf{g}^T(t) \hat{\mathbf{S}} \mathbf{g}(t) + \mathbf{h}^T(t) \hat{\mathbf{S}} \mathbf{h}(t) + \mathbf{y}^T(t) \mathbf{y}(t) < 0 \end{aligned} \quad (31)$$

Hence

$$\mathbf{y}^T(t) \mathbf{y}(t) < -\dot{V}(\hat{\mathbf{x}}(t)) + \mathbf{g}^T(t) \hat{\mathbf{S}} \mathbf{g}(t) - \mathbf{h}^T(t) \hat{\mathbf{S}} \mathbf{h}(t) \quad (32)$$

Integrating both sides of Eq. (32) over time 0 to  $\infty$ , we have

$$\int_0^\infty \mathbf{y}^T(t) \mathbf{y}(t) dt < -\int_0^\infty \dot{V}(\hat{\mathbf{x}}(t)) dt + \int_0^\infty \mathbf{h}^T(t) (\Delta^T \hat{\mathbf{S}} \Delta - \hat{\mathbf{S}}) \mathbf{h}(t) dt \quad (33)$$

Recalling  $\|\Delta\| \leq 1$ , and  $\|w_0\| \leq 1$ , we have

$$\int_0^\infty \mathbf{y}^T(t) \mathbf{y}(t) dt < V(\hat{\mathbf{x}}(0)) = \left\| \mathbf{B}_{cw}^T \hat{\mathbf{P}} \mathbf{B}_{cw} \right\| \quad (34)$$

Therefore, the fitness function Eq. (21) can be written as

$$f(j) = M - \left\| \mathbf{B}_{cw}^T \hat{\mathbf{P}} \mathbf{B}_{cw} \right\| \quad (35)$$

#### 4.4 Selection

The operation of selection can insert the best chromosome into the new population, i.e., selecting the best individual for reproduction. This can keep the best individual, evaluated by the fitness values for genetic operation, in the new generation. In the selection operation, the best individual is saved and the remainder will be probabilistically selected by the fitness values.

#### 4.5 Crossover

The crossover and mutation operation can generate new offspring generations. The probability of crossover is  $p_c$ . The cross-over arithmetic operators are defined as follows (Fogel 1994).

$$P_1^* = (1-\alpha)P_1 + \alpha P_2, \quad P_2^* = \alpha P_1 + (1-\alpha)P_2 \quad (36)$$

where,  $\alpha$  is a uniformly distributed random variable between 0 and 1,  $P_1, P_2$  are the parents, and  $P_1^*, P_2^*$  are the offspring.

#### 4.6 Mutation

The mutation operation is performed with the probability  $p_m$ . In the mutation, the offspring is randomly selected from the given parent by using the following two possibilities (Tavakolpour *et al.* 2010)

$$P_j^* = \begin{cases} P_j + 0.5\delta(P_U - P_L) & d = 0 \\ P_j - 0.5\delta(P_U - P_L) & d = 1 \end{cases}, \quad \delta = \left( \frac{G_U - G_C}{G_U} \right)^s \quad (37)$$

where  $P_j, P_j^*$  is the child and parent solution, and  $P_U, P_L$  is the upper and lower limit of the solution space.  $G_U$  is the specified maximum number of generations,  $G_C$  is the current number of generations, and  $s$  is a given positive number.

#### 4.7 Termination

The condition for terminating the genetic algorithm generation loop could be either when the desired accuracy has been achieved or when a certain number of generations have been reached. The maximum number of generations is set as the terminating condition in this work, i.e., the optimal process will be stop when the allowable generation number has been reached. It is worth noting that results obtained from a genetic algorithm process with the limited number of generation might be a suboptimal solution. To get a result with higher confidence, one has to run the genetic process either several times, each with a randomly generation initial condition satisfying the robust stability and disturbance rejection conditions Eq. (19), or with sufficient number of generations.

### 5. Numerical example

Here consider the flexural vibration control of a simply supported beam with non-collocated piezoelectric actuator/sensor patches bonded to it. The beam has the geometric parameters of

length (0.5 m), thickness (0.01 m) and width (0.05 m) and the material properties of Young's elastic modulus (70 GPa) and mass density (2500 kg/m<sup>3</sup>). The disturbance is assumed to enter through the actuator channel. The damping ratio of all modes is assumed to be 0.005; The material properties of the piezoelectric actuator/sensor are as follows:  $d_{31}=120\times 10^{12}$  m/V,  $g_{31}=-1.15\times 10^{-2}$  Vm/N,  $C_p=1.05\times 10^{-7}$  F,  $E_p=63$  GPa. The width of the piezoelectric actuator/sensor is the same as that of the beam, and their thickness is  $2\times 10^{-4}$  m. The piezoelectric actuator patch is located at  $0.23l_b\rightarrow 0.49 l_b$  along the beam ( $l_b$  is the length of the beam), while the piezoelectric sensor is located at  $0.58l_b\rightarrow 0.85 l_b$ . The performance displacement output is the displacement coming from a point along the beam. The first four modes are considered in the control design stage. The high-frequency modes is considered as norm-bound additive uncertainty, which is normalized by weighting function  $W(s)=0.01s^2/(1+s/8)^2$  (from actuator to performance output); The genetic algorithm optimization is used to seek the best controller parameters. Crossover probability  $p_c=0.6$  and probability of mutation  $p_m=0.004$ . The maximum number of generations is set as 50 with the initial populations  $P_j=\{\mathbf{A}_k, \mathbf{B}_k, \mathbf{C}_k\}$ ,  $j=1,2,\dots,10$  generated by the designing of 10 suboptimal controllers. The mixed controller parameters  $\mathbf{A}_k, \mathbf{B}_k, \mathbf{C}_k$  are as follows

$$\mathbf{A}_k = \begin{bmatrix} -0.0383 & 1.3485 & -0.8833 & -2.5985 & 0.1973 & -1.3870 & -0.7963 & -5.5726 & 0.8755 & 7.8593 \\ 0.0020 & -4.4520 & 3.4709 & 3.5671 & -1.8762 & 2.2669 & 0.4855 & 8.6432 & -0.7026 & -2.0205 \\ -0.0318 & 0.6828 & -0.7429 & -2.9102 & 0.6232 & -0.9427 & -0.5862 & -3.1158 & 0.0554 & 3.7600 \\ 0.0617 & 1.4664 & -2.4326 & 11.4574 & -4.5713 & 7.9810 & 1.5673 & 13.5986 & -0.6324 & 3.9600 \\ -0.0083 & 0.1994 & -0.1752 & -0.3027 & -0.2172 & -0.0285 & 1.2145 & -0.3623 & 0.5091 & -0.0757 \\ -0.0206 & 0.5722 & -0.1905 & -0.9902 & -0.1671 & -0.6109 & 1.2618 & -1.5158 & -0.8991 & -0.8502 \\ -0.0034 & -1.9618 & 0.6547 & -1.2964 & 0.3864 & -0.8252 & 0.3840 & -1.4978 & -0.0218 & -0.9530 \\ 0.0364 & 1.0078 & -1.4491 & 1.3349 & 0.2190 & -0.1580 & 0.3175 & 1.8556 & -0.4527 & -5.3395 \\ -0.1876 & -0.3805 & 0.2449 & -0.0489 & -6.2166 & 1.9123 & -2.6766 & -4.4926 & 2.9730 & 50.9036 \\ 0.0350 & 0.3711 & -0.2639 & -0.4452 & 1.3122 & -0.6077 & 0.5139 & 0.1630 & -0.6182 & -9.9320 \end{bmatrix}$$

$$\mathbf{B}_k = [2.4424 \quad -6.6585 \quad 3.0960 \quad -3.2140 \quad 4.9901 \quad 4.0383 \quad -1.3757 \quad 0.5712 \quad -0.5429 \quad 1.7315]^T$$

$$\mathbf{C}_k = [0.0925 \quad 0.0032 \quad 0.0001 \quad -0.0263 \quad -0.0026 \quad -0.0221 \quad -0.0059 \quad -0.0313 \quad 0.0019 \quad 0.1953]$$
(38)

Compared to the robust  $H_\infty$  method, the impulse responses and frequency responses for the controlled system are shown in the Fig. 2 and Fig. 3 respectively. In these two figures, the mixed control exhibits better time-domain performance, having a settling time of 132s, which is less than that of the pure  $H_\infty$  control with a settling time of 139s. The pure  $H_\infty$  control exhibits a better frequency-domain performance, having a maximum attenuation of approximate 32.94 dB in terms of vibration magnitude, than mixed control with a maximum attenuation of approximate 30.34 dB.

The impulse responses and frequency responses for the controlled system, as compared to the robust  $H_2$  method are shown in the Fig. 4 and Fig. 5, respectively. In these two figures, the mixed control exhibits a better frequency-domain performance, having a maximum attenuation of 30.34 dB, which is better than that of a pure  $H_2$  control with a maximum attenuation of 24.85 dB. Please note that the pure  $H_2$  control exhibits better time-domain performance, having a settling time of 127 s, which is less than that of the mixed control with a settling time of 132 s.

For comparative purpose, both velocity feedback control, which is effectively used in active vibration control by modifying the damping of the system and consequently the closed-loop poles (Kapuria and Yaqoob 2010, Bodaghi *et al.* 2012), and the mixed control are employed to control

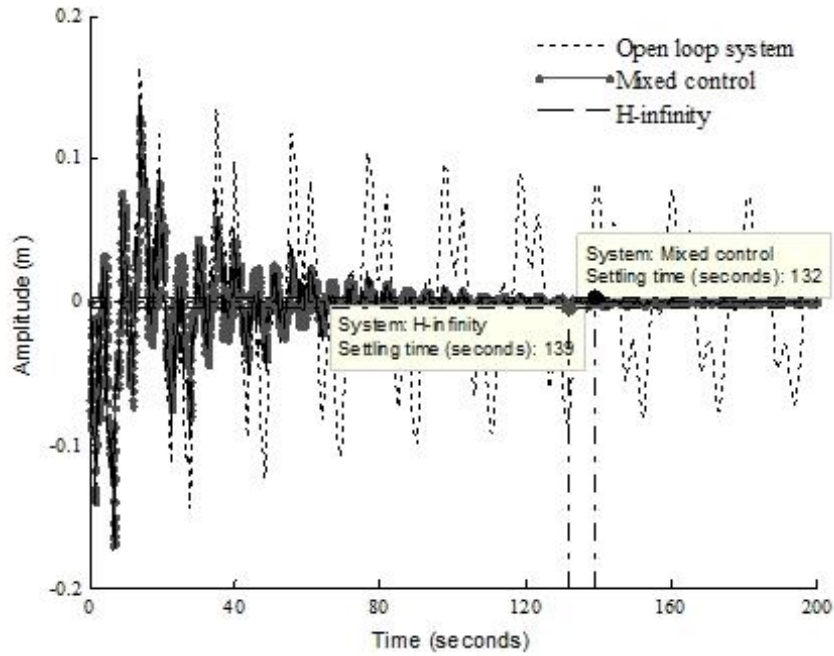


Fig. 2 Impulse responses for systems (H-infinity control and mixed control)

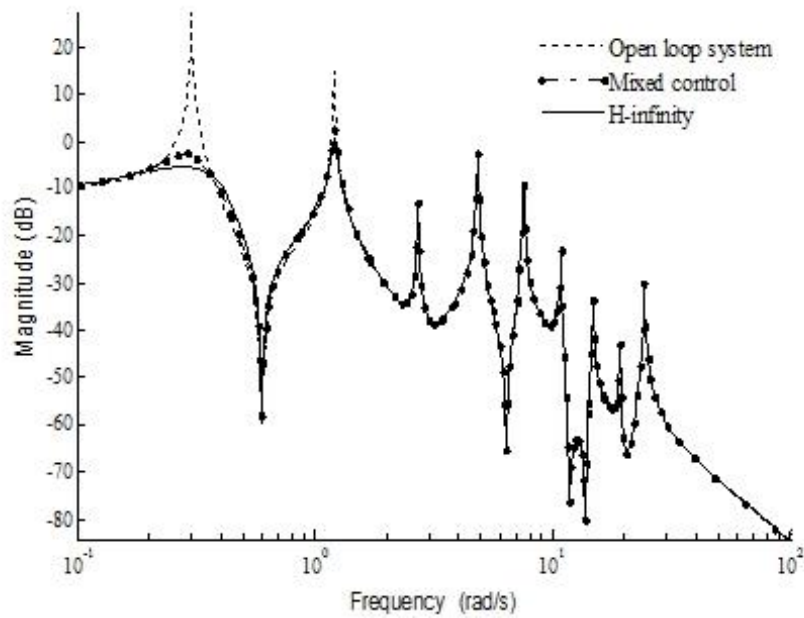


Fig. 3 frequency responses for systems (H-infinity control and mixed control)

the vibration of the flexible beam mentioned above. In velocity feedback control, the control law can be expressed as (Kapuria and Yaqoob 2010)

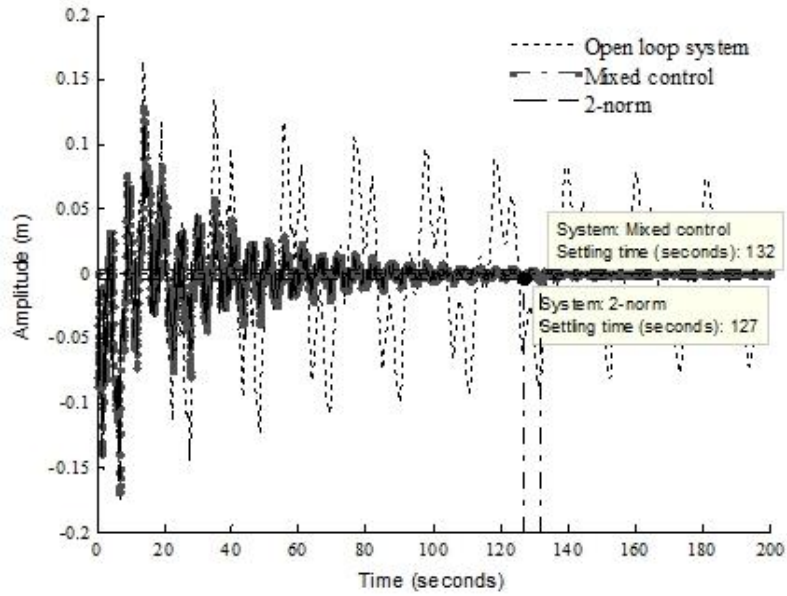


Fig. 4 Impulse responses for systems (2-norm control and mixed control)

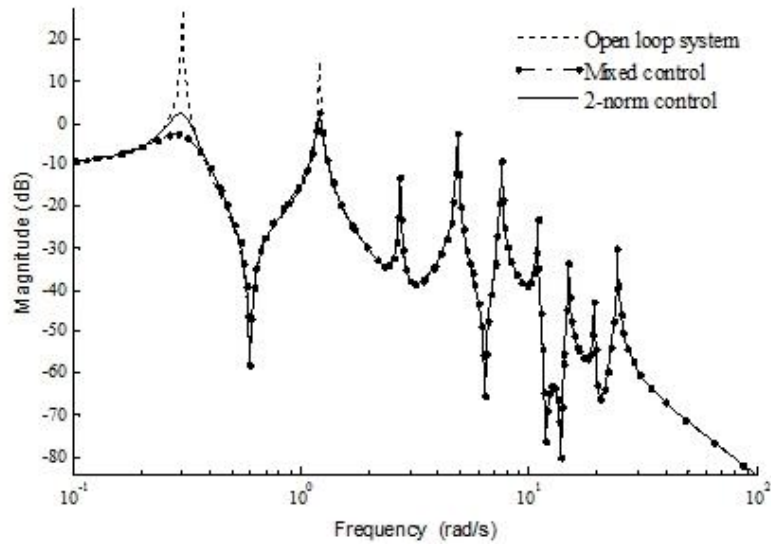


Fig. 5 Frequency responses for systems (2-norm control and mixed control)

$$\begin{aligned}
 \mathbf{V}_a(t) &= -\mathbf{Gz}(t), \quad \mathbf{G} = \begin{bmatrix} \mathbf{0} & \mathbf{G}_v \end{bmatrix} \\
 \mathbf{z}(t) &= \hat{\mathbf{C}}\mathbf{X}(t)
 \end{aligned}
 \tag{39}$$

where,  $\mathbf{G}_v$  is the velocity gain matrix.

The impulse responses and frequency responses for the controlled system, as compared to the

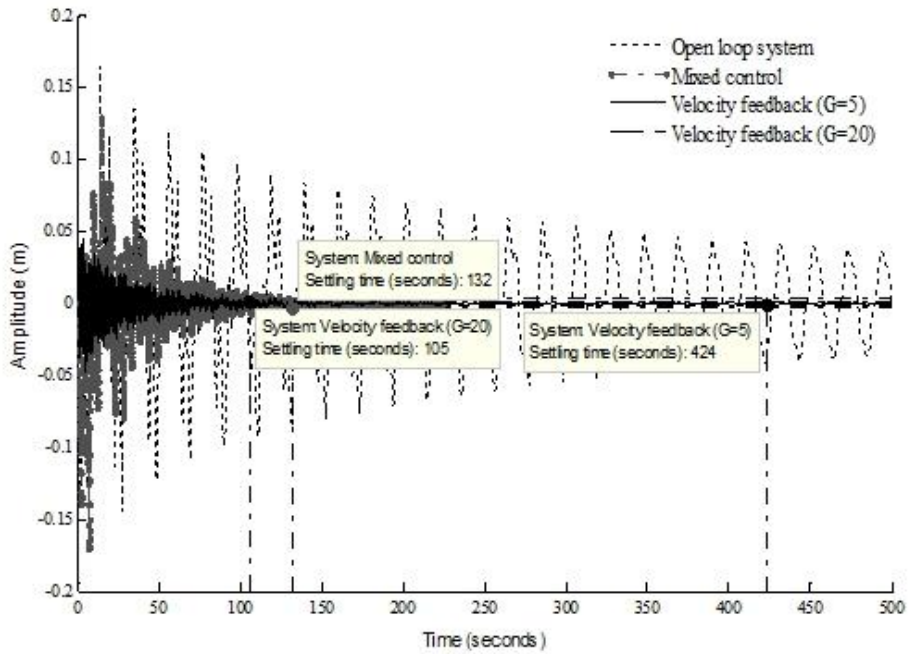


Fig. 6 Impulse responses for systems (velocity feedback control and mixed control)

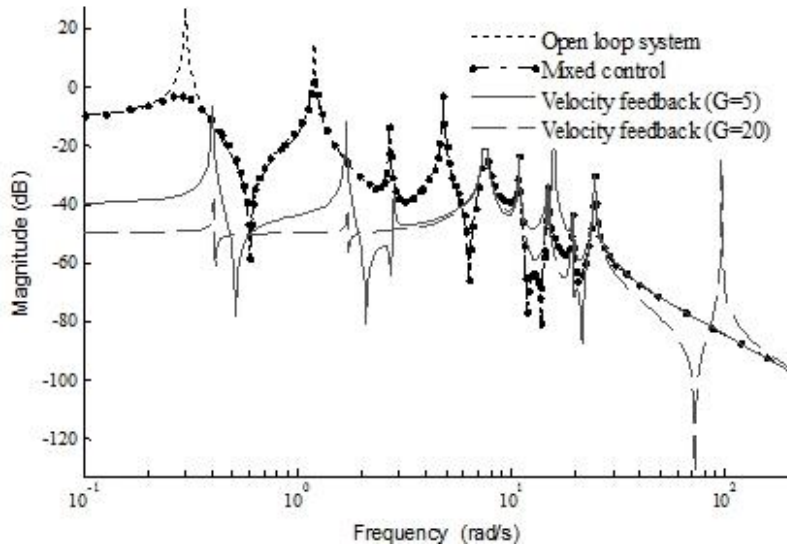


Fig. 7 Frequency responses for systems (velocity feedback control and mixed control)

velocity feedback control method, are shown in the Fig. 6 and Fig. 7, respectively. It can be seen from Fig. 6 that the velocity control with a large gain exhibits better time-domain performance, having a settling time of 105 s for  $G=20$ , which is better than those of both mixed control with a settling time of 132 s and the small-gain velocity feedback control with a settling time of 424 s for  $G=5$ . It is observed from Fig. 7 that the mixed control law can suppress the low-frequency modes

without exciting the high-frequency modes, while the velocity feedback control method, which performs well in time-domain and low-frequency domain, excites the un-modeled high-frequency modes and may degrade the performance in the high-frequency domain for the non-collocated system.

It is pertinent to mention that although a simple supported beam is used for discussion, the general procedure for controller design proposed in this paper applies to more complex structures, such as plates and shells, after the stochastic finite element models are developed and modal analysis is conducted to include the uncertain dynamics in the modal space.

## 6. Conclusions

In the vibration control,  $H$ -infinity norm focuses on the case that the vibration is excited at the fundamental frequency, and 2-norm weighs the overall performance of a system with the input of pulses or white noises. Using LMI and genetic algorithm, a dynamical output feedback control law with best controller parameters is designed by not only minimizing  $H_2$  norm but also setting an upper bound on  $H_\infty$  norm to suppress the vibration of an uncertain piezoelectric flexible beam structure due to external disturbances. In the optimization processing of genetic algorithm, the robust  $H_2$  performance of the closed-loop system with norm-bound uncertainty is included in the fitness function.

The simulation results show that mixed control method based on LMI and genetic algorithm with the proposed fitness function provides the remarkable flexibility to comprise between frequency-domain performance and time-domain performance while the pure  $H_\infty$  control method possesses better robust frequency-domain performance, having smaller peak frequency response, and pure  $H_2$  control method possesses better time-domain performance, having shorter settling time of impulse response. Compared to the velocity feedback control method in literatures which is easier to implement practically because of more simple control structure and exhibits excellent control performance in time-domain and low-frequency domain, the proposed control law can suppress the low-frequency modes without exciting the high-frequency modes.

## References

- Belouettar, S. and Azrar, L. (2008), "Active control of nonlinear vibration of sandwich piezoelectric beams: A simplified approach", *Comput. Struct.*, **86**, 386-397.
- Balas, M.J. (1978), "Feedback control of flexible systems", *IEEE T. Automat. Contr.*, **23**(4), 673-679.
- Bala, G.L. (1995), "Control design for variation in structural natural frequencies", *J. Guid. Contr. Dyn.*, **18**(2), 325-332.
- Bodaghi, M., Damanpack, A.R., Aghdam, M.M. and Shakeri, M. (2012), "Non-linear active control of FG beams in thermal environments subjected to blast loads with integrated FGP sensor/actuator layers", *Compos. Struct.*, **94**, 3612-3623.
- Bruant, I. and Gallimard, L. (2010), "Optimal piezoelectric actuator and sensor location for active vibration control, using genetic algorithm", *J. Sound Vib.*, **329**, 1615-1635.
- Caracciolo, D., Richiedei, D. and Trevisani, A. (2005), "Robust mixed-norm position and vibration control of flexible link mechanisms", *Mechatronics*, **15**, 767-791.
- Chen, S.H., Song, M. and Dong, Y. (2007), "Robustness analysis of responses of vibration control structures with uncertain parameters using interval algorithm", *Struct. Saf.*, **29**, 94-111.

- Damanpack, A.R., Bodaghi, M., Aghdam, M.M. and Shakeri, M. (2013), "Active control of geometrically non-linear transient response of sandwich beams with a flexible core using piezoelectric patches", *Compos. Struct.*, **100**, 517-531.
- Fogel, D.B. (1994), "An introduction to simulated evolutionary optimization", *IEEE T. Neural Networ.*, **5**(1), 3-14.
- Gao, W. and Chen, J.J. (2003), "Optimal placement of active bars in active vibration control for piezoelectric intelligent truss structures with random parameters", *Comput. Struct.*, **81**(1), 53-60.
- Gawronski, W. (1996), *Balanced Control of Flexible Structures*, Berlin, Springer.
- Gasbarri, P., Monti, P. and Sabatini, M. (2014), "Very large space structures: Non-linear control and robustness to structural uncertainties", *Acta Astronaut.*, **93**, 252-265
- Karimi, H.R., Zapateiro, M. and Luo, N.S. (2008), "Robust mixed  $H_2/H_\infty$  delayed state feedback control of uncertain neutral systems with time-varying delays", *Asian J. Control*, **10**(5), 569-580.
- Kapuria, S. and Yaqoob, Y.M. (2010), "Active vibration control of piezoelectric laminated beams with electroded actuators and sensors using an efficient finite element involving an electric node", *Smart. Mater. Struct.*, **19**, 5004-5019.
- Lin, J. and Zheng, Y.B. (2012), "Vibration suppression control of smart piezoelectric rotating truss structure by parallel neuro-fuzzy control with genetic algorithm tuning", *J. Sound Vib.*, **331**, 3677-3694.
- Meirovitch, L. and Baruh, H. (1983), "A comparison of control techniques for large flexible systems", *J. Guid. Contrl Dyn.*, **6**(4), 302-310.
- Morales, A.L., Rongong, J.A. and Sims, N.D. (2012), "A finite element method for active vibration control of uncertain structures", *Mech. Syst. Signal Pr.*, **32**, 79-93.
- Qiu, Z.Q. and Wu, H.X. (2009), "Acceleration sensors based modal identification and active vibration control of flexible smart cantilever plate proportional feedback control", *Aeros. Sci. Tech.*, **13**, 277-290.
- Tavakolpour, A.R., MatDarus, I.Z. and Tokhi, O. (2010), "Genetic algorithm-based identification of transfer function parameters for a rectangular flexible plate system", *Eng. Appl. Artif. Intel.*, **23**, 1388-1397.
- Rittenschober, T. and Schlacher, K. (2012), "Observer-based self sensing actuation of piezoelastic structures for robust vibration control", *Automatica*, **48**(6), 1123-1131
- Samuel, D.S. and Vicente, L.J. (2006), "Design of a Control System using Linear Matrix Inequalities for the Active Vibration Control of a Plate", *J. Intel. Mat. Syst. Struct.*, **17**(1), 81-93.
- Sana, S. and Rao, V.S. (2000), "Application of linear matrix inequalities in the control of smart structural systems", *J. Intel. Mat. Syst. Struct.*, **11**, 321-323.
- Schulz, S.L., Gomes, H.M. and Awruch, A.M. (2013), "Optimal discrete piezoelectric patch allocation on composite structures for vibration control based on GA and modal LQR", *Comput. Struct.*, **128**, 101-115.
- Song, G. and Sethi, V. (2006), "Vibration control of civil structures using piezoceramic smart materials: A review", *Eng. Struct.*, **28**, 1513-1524.
- Tavakolpour, A.R., Mailah, M. and Darus, I.Z. (2010), "Self-learning active vibration control of a flexible plate structure with piezoelectric actuator", *Simul. Model. Pract. Theory*, **18**, 516-532.
- Vasques, C.M.A. and Rodrigues, J.D. (2006), "Active vibration control of smart piezoelectric beams: Comparison of classical and optimal feedback control strategies", *Comput. Struct.*, **84**, 1402-1414.
- Xu, B. and Ou, J.P. (2013), "Integrated optimization of structural topology and control for piezoelectric smart plate based on genetical algorithm", *Finite Eleme. Anal. Des.*, **64**, 1-12.
- Xu, Y.L. and Chen, J.J. (2008), "Modal-based model reduction and vibration control for uncertain piezoelectric flexible structures", *Struct. Eng. Mech.*, **29**(5), 489-504.
- Yang, C.D. and Sun, Y.P. (2002), "Mixed  $H_2 / H_\infty$  state-feedback design for microsatellite attitude control", *Control Eng. Pract.*, **10**, 951-970.
- Zhang, X. and Shao, C. (2001), "Robust  $H_\infty$  vibration control for flexible linkage mechanism systems with piezoelectric sensors and actuators", *J. Sound Vib.*, **243**, 145-155.